Entropy Generation of Unsteady MHD Couette Flow through Vertical Microchannel with Hall and Ion Slip Effects

Abiodun A. Opanuga, *Member, IAENG,* Samuel O. Adesanya, *Member, IAENG,* Sheila A. Bishop, Hilary I. Okagbue, Olasumbo O. Agboola, *Member, IAENG*

***Abstract*—In this work, the entropy generation of unsteady hydromagnetic Couette flow through vertical microchannel has been considered, the effects of Hall current and Ion-slip are also examined. One of the plates moves with uniform velocity in the direction of the fluid flow while the other plate is stationary. The partial differential equations governing the flow are obtained and transformed to ordinary differential equations. The obtained solutions for the velocity and energy equations via differential transform technique are used to calculate the entropy generation and Bejan number. The results are presented through plots and discussed. It is noticed that primary velocity decreases with increase in Hall current, ion-slip and magnetic field parameters whereas it increases as rarefaction parameter, wall-ambient temperature difference ratio, Brinkman number and Grashof number increase in values. Also secondary velocity receives a boost with increase in Hall current, Ion-slip, rarefaction parameters, wall-ambient temperature difference ratio, Brinkman and Grashof numbers. Furthermore, entropy generation is minimised as Hall current, Ion-slip and rarefaction parameters increase.**

***Index Terms*— Couette flow, Bejan number, entropy generation, differential transform method (DTM), vertical microchannel.**

I. INTRODUCTION

In fluid dynamics, Couette flow refers to flow between two parallel plates in which one of the plates is moving with uniform velocity and the other one held at rest. It was so named in honour of Maurice Marie Alfred Couette who was a Physics Professor at the French University of Angers [1]. Couette flow has applications in engineering, hydrodynamic lubrication, polymer and food processing. Specifically it is applicable in power generating industries where electric energy is produced directly from a moving conducting fluid, plasma industries, nuclear power plants, gas turbines etc. Research work in this direction has been tremendous in view of its significance resulting in the investigation of such flow by numerous researchers. These include Couette flow in horizontal parallel plates [2], Couette flow in vertical parallel plates [3], hydromagetic Couette flow [4-5], Hall-hydromagnetic Couette flow [6-10], unsteady Couette flow [11-12], mixed convection Couette flow [13-14] and reactive Couette flow [15-17].

The subject of Microchannel flow has become a popular area of research in the past few decades due to its applications in areas such as medical and biomedical fields, computer chips and chemical separations, cooling of electronic devices, micro air vehicles (MAV), micro heat exchanger systems, micro-channel heatsink, microjet impingement cooling, micro heat pipe and aircraft intake de-icing. The unique feature of this type of fluid is that the heat dissipated per unit area is directly proportion to the size of the devices; hence the performance of these devices is temperature dependent. In view of this fact, it is pertinent to study the heat transfer characteristics of such fluid flow for accurate prediction of performance during the design process. The Knudsen number (kn) which has been used to classify different flow regimes in microchannel flow is an important quantity, it is the ratio of the molecular mean free path to the characteristic length. Mention may be made of the research studies by authors such as, Weng and Chen [18] who investigated variable physical properties in natural convective gas microflow. Adesanya [19] considered velocity slip and temperature jump effects on free convective vertical porous flow of heat generating fluid. Jha et al. [20] studied suction/injection effect on natural convection flow in vertical Micro-channel. Other related works to this present study are found in the following refs. [21-26].

However, entropy generation is encountered in many energy-related systems and designs, such as microchannel flow devices; and entropy generation diminishes the available work in any system. Factors such as heat transfer, dissipations, radiation, magnetic field etc. are responsible for fluid irreversibility. Since efficient utilization of energy is the principal goal in the design of any system, therefore when factors responsible for entropy generation are determined it will help to upgrade the performance of many industrial and engineering systems and devices. Bejan [27], demonstrated that entropy generation analysis minimization can be accomplished by the application of second law of thermodynamics. Several investigations have been conducted by other researchers to affirm that some flow pertinent parameters can be analyzed to minimize entropy production in any system. Das and Jana [28] studied slip effect on the entropy generation due to MHD flow. Arikoglu

Manuscript received February, 2019; revised October 31, 2019. This work was supported by Covenant University Centre for Research and Innovation (CUCRID). A.A. Opanuga, S.A. Bishop, H.I. Okagbue and O.O. Agboola are with the Department of Mathematics, Covenant University, Ota, Nigeria (e-mail: abiodun.opanuga@covenantuniversity.edu.ng,shiela.bishop@covenantuniversity.edu.ng,hilary.okagbue@covenantuniversity.edu.ng,ola.agboola@covenantuniversity.edu.ng).

S.O. Adesanya is with the Department of Mathematics, Redeemer's University, Ede, Nigeria. (e-mail: adesanyaolumide@yahoo.com).

et al. [29] considered the effect of slip on entropy generation in a single rotating disk in MHD flow. Adesanya and Makinde [30] investigated couple stress irreversibility analysis along an inclined heated plate with adiabatic free surface. Also MHD third grade fluid irreversibility analysis through porous medium was presented by Adesanya and Falade [31]. Others are Ajibade et al. [32], Bouabid et al. [33], Rashidi and Freidoonimehr [34] and recently Opanuga et al. [35-38]. The aim of this study is the application of second law analysis to vertical microchannel Couette flow with Hall and Ion-slip effects. To the best of authors' knowledge, no studies have been presented exclusively on the entropy generation analysis of hydromagnetic vertical microchannel Couette flow with Hall and ion-slip effects.

Several techniques have been recorded in literature for solving various models arising from fluid flows. These include techniques such as Revised Variational Iteration Method [39], Laplace-Adomian Pade Method [40], Homotopy Perturbation Technique [41] and Finite Difference Technique [42]. However in this work Differential Transform Technique is applied due to its rapid convergence and simplicity in handling linear and non-linear models.

The rest of the paper is organised as follows: section 2 consists of model formulation, section 3 is devoted to differential transform solution, results and discussion are given in section 4 while section 5 is for the conclusion.

II. ANALYSIS OF MODEL

An unsteady hydrodynamic viscous incompressible Couette flow of electrically conducting fluid past an infinite vertical microchannel plate in the presence of a uniform transverse magnetic field separated by a distance h is considered. Both the fluid and channel rotate in unison about an axis normal to the plates with a uniform angular velocity Ω^*. A Cartesian co-ordinates system with x-axis vertically upward along the plate in the flow direction is chosen, the z-axis is perpendicular to the plate and the y-axis normal to xy-plane, see Fig. 1. It is assumed that one of the plates moves with a constant velocity in the flow direction in the presence of a transverse magnetic field while the other is stationary. It is further assumed that relatively high electron-atom collision frequency is strong so that the effects of Hall current and ion slip are significant. The plates are asymmetrically heated with one plate maintained at a temperature T_1 while the other plate is at a temperature T_2 such that $T_1 > T_2$. The flow is fully developed hydrodynamically and thermally, therefore the fluid velocity and the temperature in the channel are functions of y only. The governing equations for the fluid flow in the presence of velocity slip and temperature jump under Boussinesq's approximation are obtained as follows:

$$\frac{\partial v}{\partial y} = 0 \tag{1}$$

$$\frac{\partial u}{\partial t} + v\frac{\partial u}{\partial y} - 2\Omega^* w = \nu\frac{\partial^2 u}{\partial y^2} + g^*\beta(T - T_0) - \frac{\sigma B_0^2}{\rho(1+m^2)}(u + mw) \tag{2}$$

$$\frac{\partial w}{\partial t} + v\frac{\partial w}{\partial y} + 2\Omega^* u = \nu\frac{\partial^2 w}{\partial y^2} + \frac{\sigma B_0^2}{\rho(1+m^2)}(mu - w) \tag{3}$$

$$\frac{\partial T}{\partial t} + v\frac{\partial T}{\partial y} = \frac{k}{\rho C_p}\frac{\partial^2 u}{\partial y^2} + \frac{\mu}{\rho C_p}\left[\left(\frac{\partial u}{\partial y}\right)^2 + \left(\frac{\partial w}{\partial y}\right)^2\right] + \frac{\sigma B_0^2}{\rho C_p(1+m^2)}(u^2 + w^2) \tag{4}$$

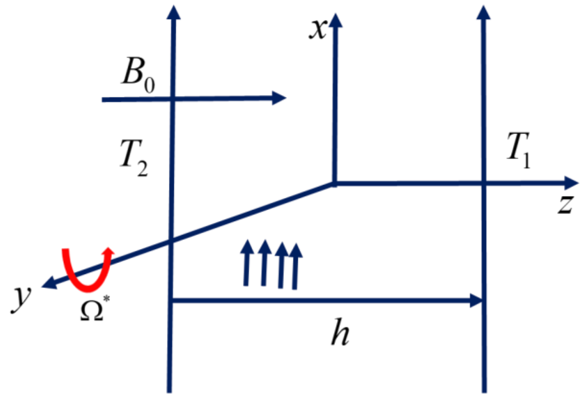

Fig 1: Flow Configuration

Introducing the following time-independent similarity and dimensionless variables,

$$\eta = \frac{y}{2\sqrt{\nu t}}, u = Uf(\eta), w = Ug(\eta), \theta(\eta) = \frac{T - T_0}{T_1 - T_0},$$
$$\Pr = \frac{\nu}{\alpha}, v = -c\sqrt{\frac{\nu}{t}}, K = 8\Omega^* t, Gr = \frac{4g^*\beta t(T_w - T_0)}{U},$$
$$H^2 = \frac{4\sigma B_0^2 t}{\rho}, Br = \frac{\mu U^2}{kh^2(T_2 - T_0)}, \beta_v = \frac{2 - F_v}{F_v}, \tag{5}$$
$$\beta_t = \frac{2 - F_t}{F_t}\frac{2\gamma_s}{\gamma_s + 1}\frac{1}{\Pr}, \gamma_s = \frac{c_p}{c_v}, Kn = \frac{\lambda}{b},$$
$$\xi = \frac{T_2 - T_0}{T_1 - T_0}, In = \frac{\beta_t}{\beta_v}$$

equations (2)-(4) reduce to

$$f'' + 2(\eta + c)f' - K^2 g + Gr\theta - \frac{H^2}{(1+m^2)}(f + mg) = 0 \tag{6}$$

$$g'' + 2(\eta + c)g' + K^2 f + \frac{H^2}{(1+m^2)}(mf - g) = 0 \tag{7}$$

$$\theta'' + 2\Pr(\eta + c)\theta' + Br\left[(f')^2 + (g')^2\right] + \frac{H^2}{(1+m^2)}(f^2 + g^2) = 0 \tag{8}$$

The dimensionless boundary conditions that describe the slip velocity and temperature jump at fluid-wall interface are [43]

$$\left.\begin{array}{l} f(0)=\beta_V Knf'(0), g(0)=\beta_V Kng'(0), \\ \theta(0)=\xi+\beta_v Kn\ln\theta'(0),\ f(1)=-\beta_V knf'(1), \\ g(1)=-\beta_V Kng'(1), \theta(1)=1-\beta_v Kn\ln\theta'(1) \end{array}\right\} \tag{9}$$

where B_0^2 is the Uniform transverse magnetic field, u, w are velocity components, f, g are dimensionless velocity, U is the characteristic velocity, h is channel width, F_t, F_v are thermal and tangential momentum accommodation coefficients, respectively, $\ln$ is fluid–wall interaction parameter, K is rotation parameter, k is coefficient of thermal conductivity, kn is Knudsen number, m is Hall current parameter, H is Hartmann number, $\Pr$ is Prandtl number, T is fluid temperature, T_0 is reference temperature, Br is Brinkman number, c is suction parameter, λ is molecular mean free Path, g^* is acceleration due to gravity, E_G is local volumetric entropy generation rate, Be is Bejan number, C_p, C_v are specific heats at constant pressure and volume respectively, Ns is dimensionless entropy generation parameter, ρ is fluid density, β_t, β_v, are dimensionless variables, γ_s is ratio of specific heats, μ is coefficient of viscosity, ξ is wall-ambient temperature difference ratio, σ is electrical conductivity, Ω is temperature difference, Ω^* is angular velocity, β is coefficient of thermal expansion and α is thermal diffusivity.

III. SOLUTION PROCEDURE

In Table 1, the basic definitions and properties of differential transform technique relevant to this work are presented

Table 1: Operations and Properties of Differential Transform Method

Original function	Transformed function
$f(y)=u(y)\pm w(y)$	$F(n)=U(n)\pm W(n)$
$f(y)=\dfrac{d^m u}{dy^m}$	$F(n)=\dfrac{(n+m)!}{n!}U(n+m)$
$f(y)=u^2$	$F(n)=\sum_{t=0}^{n} U(t)U(n-t)$
$f(y)=\left(\dfrac{du}{dy}\right)^2$	$F(n)=\sum_{t=0}^{n} (t+1)(n-t+1) U(t+1)U(n-t+1)$

In applying DTM, the stated properties in Table 1 are invoked to transform the differential equations (6)-(8) which yield the following recursive relations:

$$F(n+2)=\frac{1}{(n+2)!}\left[\begin{array}{l} -2\eta(n+1)F(n+1)-2c(n+1) \\ F(n+1)+2K^2G(n)-Gr(n) \\ +\dfrac{H^2}{1+m^2}\left(F(n)+mG(n)\right) \end{array}\right] \tag{10}$$

$$G(n+2)=\frac{1}{(n+2)!}\left[\begin{array}{l} -2\eta(n+1)G(n+1)- \\ 2c(n+1)G(n+1)-2K^2F(n) \\ -\dfrac{H^2}{1+m^2}\left(mF(n)-G(n)\right) \end{array}\right] \tag{11}$$

$$\begin{aligned} \Theta(n+2)=\frac{1}{(n+2)!}\Bigg[&-2\Pr(n+1)\Theta(n+1)- \\ &2c\Pr(n+1)\Theta(n+1)- \\ &Br\left(\sum_{t=0}^{n}(t+1)(n-t+1)F(n-t+1)F(n-t+1)\right. \\ &\left.+\sum_{t=0}^{n}(t+1)(n-t+1)G(t+1)G(n-t+1)\right) \\ &-\frac{BrH^2}{1+m^2}\left(\begin{array}{l}\sum_{t=0}^{n}F(t)F(n-t)+ \\ \sum_{t=0}^{n}G(t)G(n-t)\end{array}\right)\Bigg] \end{aligned} \tag{12}$$

Note $F(n)$, $G(n)$ and $\Theta(n)$ are the differentially transformed functions of $f(y)$, $g(y)$ and $\theta(y)$ respectively, they are given as

$$\begin{aligned} &f(y)=\sum_{n=0}^{\infty} y^n F(n), \quad G(y)=\sum_{n=0}^{\infty} y^n G(n), \\ &\theta(y)=\sum_{n=0}^{\infty} y^n \Theta(n) \end{aligned} \tag{13}$$

The following are the initial conditions chosen based on the model

$$\begin{aligned} &F(0)=a_1, \quad F(1)=a_2, \quad G(0)=a_3, G(1)=a_4, \\ &\Theta(0)=a_5, \quad \Theta(1)=a_6 \end{aligned} \tag{14}$$

Equations (13) are substituted into equations (10)-(12) to determine the values of $F(n)$, $G(n)$ and $\Theta(n)$ for $n=0,1,\ldots,$ recursively. The values of $F(n)$, $G(n)$ and $\Theta(n)$ for $n=0,1,\ldots,$ are further substituted into equations (13) to obtain the following series solution in the form:

$$\begin{aligned} &f(y)=\sum_{n=0}^{t} y^n F(k), \quad G(y)=\sum_{n=0}^{t} y^n G(n), \\ &\theta(y)=\sum_{n=0}^{t} y^n \Theta(n) \end{aligned} \tag{15}$$

The transformed form of boundary conditions are invoked on (15) to obtain the values of all the unknown coefficients given in (14).

Finally equations (10-14) are coded in symbolic Maple software to yield the approximate solution. The results are presented in Figures 2-36.

The entropy generation for the model is given as following Bejan [27].

$$\begin{aligned} E_G=&\frac{k}{T_0^0}\left(\frac{\partial T}{\partial y}\right)^2+\frac{\mu}{T_0}\left(\left(\frac{\partial u}{\partial y}\right)^2+\left(\frac{\partial w}{\partial y}\right)^2\right)+ \\ &\frac{\sigma B_0^2}{T_0}\left(w^2+u^2\right), \end{aligned} \tag{16}$$

Using equation (5) in (16) yields

$$Ns = \theta'^2(\eta) + \frac{Br}{\Omega}\left[\left(f'(\eta)\right)^2 + \left(g'(\eta)\right)^2 + H^2\left(f^2(\eta) + g^2(\eta)\right)\right] \quad (17)$$

The ratio of heat transfer irreversibility (N_1) to fluid friction irreversibility (N_2) is stated as

$$\Phi = \frac{N_2}{N_1} \quad (18)$$

However, Bejan number gives the alternative entropy generation distribution ratio parameter; it describes the ratio of heat transfer irreversibility (N_1) to the total entropy generation (N_S) due to heat transfer and fluid friction

$$Be = \frac{N_1}{N_S} = \frac{1}{1+\Phi}, \quad \Phi = \frac{N_2}{N_1}. \quad (18)$$

and

$$Be = \begin{cases} 0, N_2 \gg N_1 \\ 0.5, N_1 = N_2 \\ 1, N_2 \ll N_1 \end{cases} \quad (19)$$

IV. RESULTS AND DISCUSSION

In this section, the description of the graphical results of some thermophysical parameters for velocity, temperature, entropy generation and Bejan number are presented. The following reference values are chosen for the computations $\Pr = 0.71, \Omega = 1, c = 0.25$ while the intervals for the parameters are $0 \le \beta v Kn \le 0.1$, $0 \le \xi \le 0.1$, $1 \le Br \le 5$, $0.5 \le K \le 1.5$, $0.1 \le m \le 0.5$, $0.4 \le H \le 2$ and $0.5 \le Gr \le 1.5$.

Validation of this present work is presented in Table 2 by comparing the exact solution and the differential transform solution of the temperature profile in equation (8).

Table 2: Comparison of exact solution and DTM solution for $\Pr = 0.71, c = 0.25, Br = 0, H = 0$

η	EXACT SOLUTION	DTM SOLUTION	ABSOLUTE ERROR
0	0.505277111	0.505277111	0
0.1	0.60198292	0.60198292	0
0.2	0.682960592	0.682960592	0
0.3	0.750768137	0.750768137	0
0.4	0.807547531	0.807547531	0
0.5	0.855092381	0.855092381	9.99201×10^{-16}
0.6	0.894904584	0.894904584	0
0.7	0.92824177	0.92824177	0
0.8	0.956157029	0.956157029	1.55431×10^{-15}
0.9	0.956157029	0.979532178	0.023375149
1	0.999105617	0.999105617	9.99201×10^{-16}

Figures 2 and 3 depict the variation in fluid primary and secondary velocity as Hall parameter takes higher values. In Hall current, there is a drift of charged particles leading to the reduction in the conductivity of current parallel to the electric field which induces current in the direction normal to both electric and magnetic fields. In view of this it is therefore observed that primary velocity decelerates while secondary velocity is enhanced. This result confirms the usual nature of Hall current which is to induce fluid flow in the secondary flow direction. Furthermore, in Figure 4 fluid temperature is unaffected by the variation in Hall current parameter, however a slight reduction in the entropy is noticed with the increasing values of Hall parameter in the entire channel as illustrated in Figure 5. Figure 6 depicts the influence of Hall current on Bejan number, it is clearly depicted that Bejan number is enhanced with increase in Hall parameter which points to the fact that heat transfer irreversibility is stronger than fluid friction irreversibility. It is noteworthy that Bejan number is not affected in the region $\eta = 0.85$ and $\eta = 0.95$.

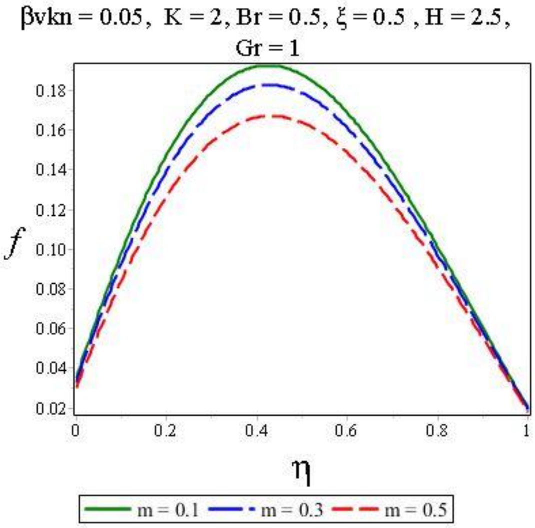

Fig 2: Primary velocity profile for various values of m

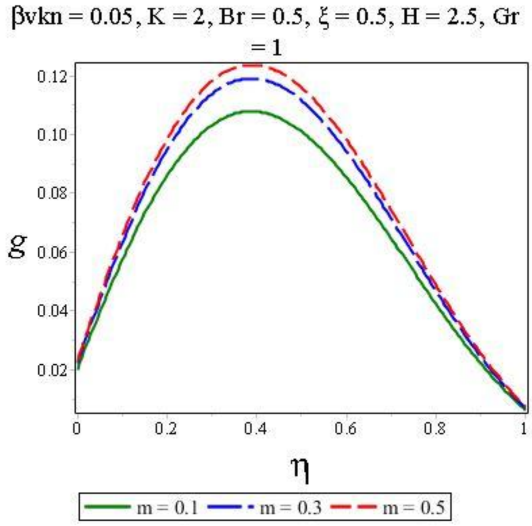

Fig 3: Secondary velocity profile for various values of m

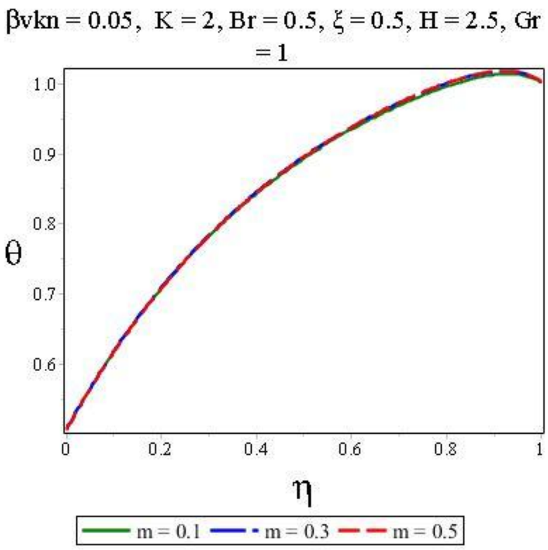

Fig 4: Temperature profile for various values of m

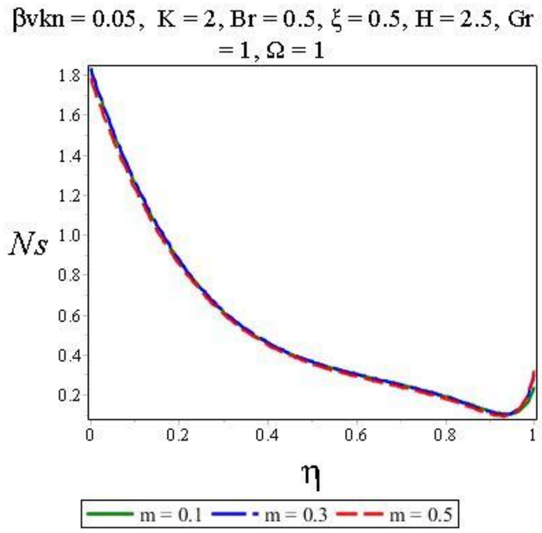

Fig 5:Entropy generation for various values of values of m

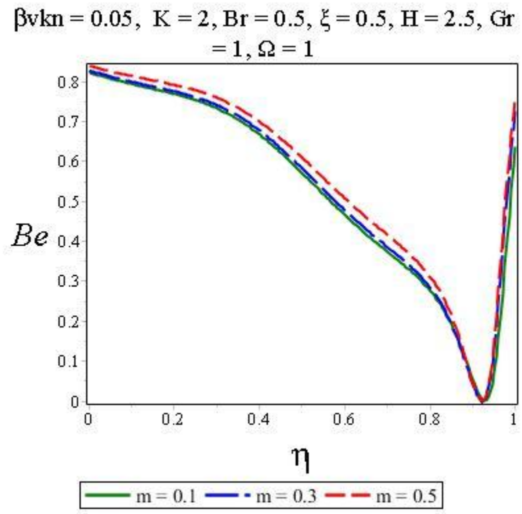

Figure 6: Bejan number for various values of m

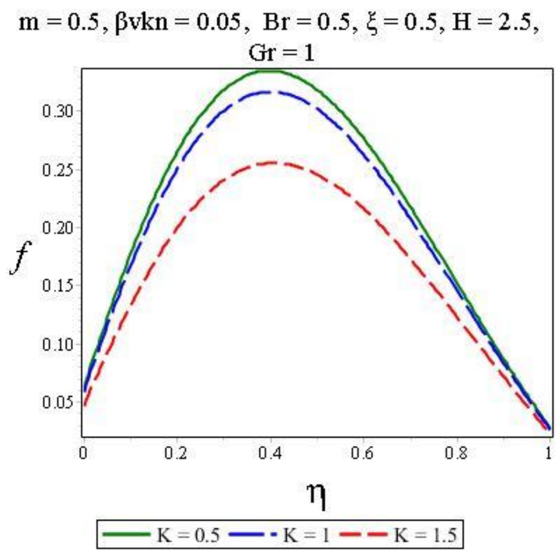

Fig 7: Primary velocity profile for various values of K

The effect of Ion-slip on fluid velocity, fluid temperature, entropy generation and irreversibility ratio is illustrated in Figures 7-11. In Figure 7 there is a significant reduction in fluid velocity as Ion-slip parameter increases while a reverse phenomenon is experienced in Figure 8. Coriolis force is responsible for such observation as it tends to reduce fluid velocity in the primary flow direction whereas it has reverse effect on the fluid velocity in the secondary flow direction. Figure 9 indicates that increase in Ion-slip parameter does not have any significant impact on fluid temperature, however the effect becomes more pronunced as the values of K increase. Entropy generation is found to reduce with increasing values of Ion-slip parameter as depicted in Figure 10, on the other hand Bejan number is enhanced almost in the entire channel except at $\eta = 0.95$. It can be deduced that fluid entropy generation is mainly contributed by heat transfer irreversibility.

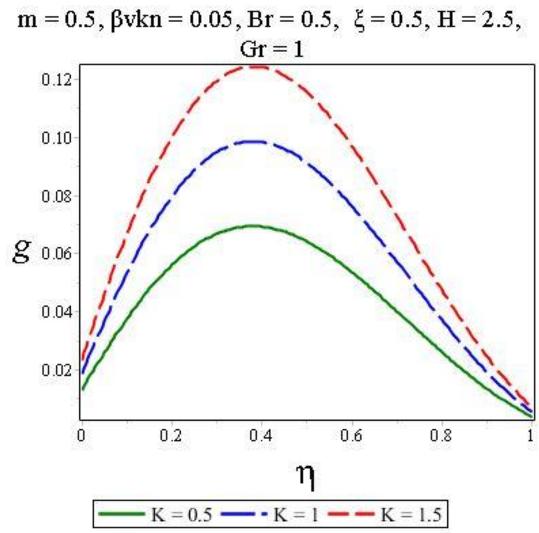

Fig 8: Secondary velocity profile for various of K

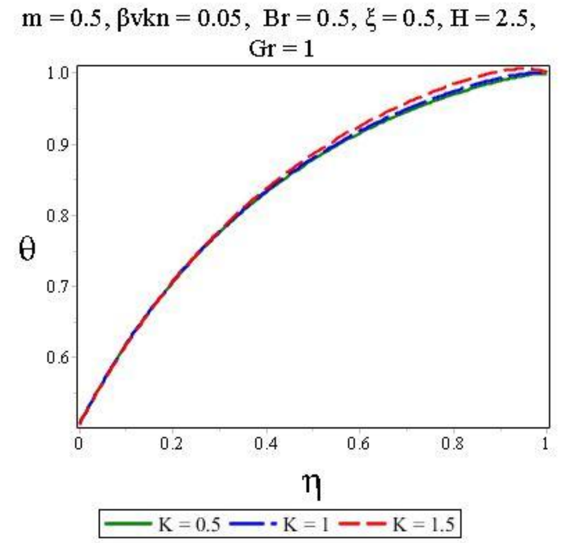

Fig 9: Temperature profile for various values of K

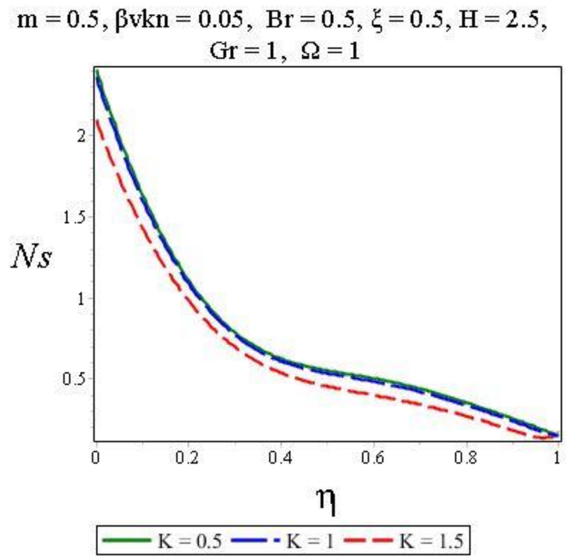

Fig 10: Entropy generation for various values of K

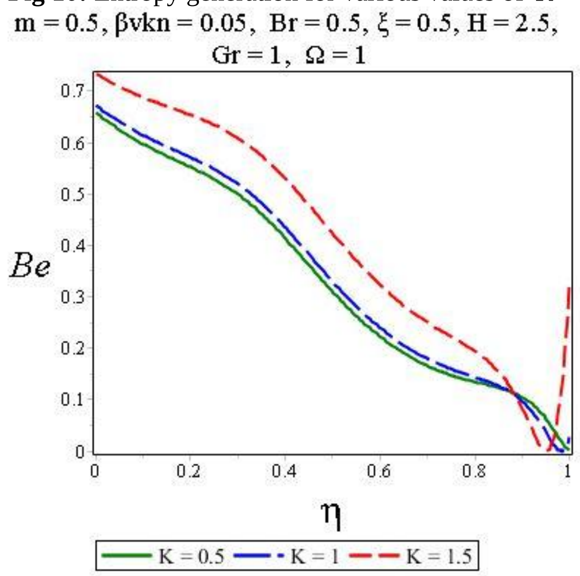

Fig 11: Bejan number for various values of K

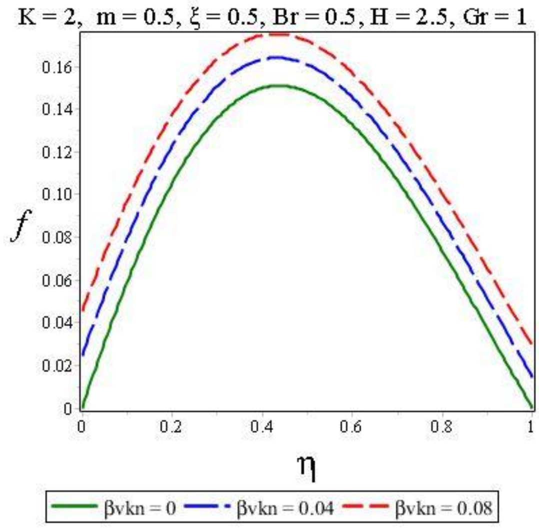

Fig 12: Primary velocity profile for various values of $\beta_V Kn$

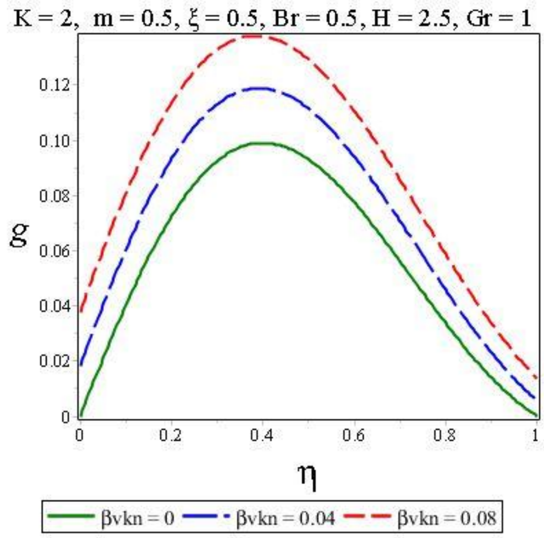

Fig 13: Secondary velocity profile for various values of $\beta_V Kn$

The influence of rarefaction parameter on fluid velocity, temperature, entropy generation and Bejan is depicted in Figures 12 to 16. It is observed in Figures 12 and 13 that fluid motion is accelerated significantly as $(\beta_V Kn)$ increases. This can be traced to the fact that a rise in the values of $(\beta_V Kn)$ accelerates fluid particles slip at the channel wall thereby discouraging the retardation effect of the wall. Furthermore, increasing the rarefaction parameter brings about an increase in the temperature jump and this reduces the amount of heat transfer from the microchannel surfaces to the fluid. In Figures 14, 15 and 16 fluid temperature, entropy generation and Bejan number are reduced as $(\beta_V Kn)$ increases. Specifically in Figure 14 the reduction is only noticed at the point $\eta > 0.3$ whereas entropy generation is experinced between $0 \geq \eta \geq 0.3$ and $\eta > 0.9$ as displayed in Figure 15. Figure 16 depicts a point where Bejan number is unaffected by the increase in the values of rarefaction parameter $(\beta_V Kn)$. It is concluded that fluid friction irreversibility becomes the major contributor to entropy generation as $(\beta_V Kn)$ takes higher values.

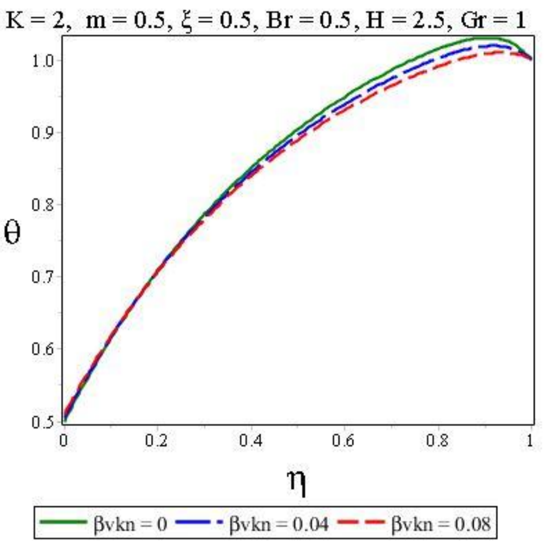

Fig 14: Temperature profile for various values of $\beta_V Kn$

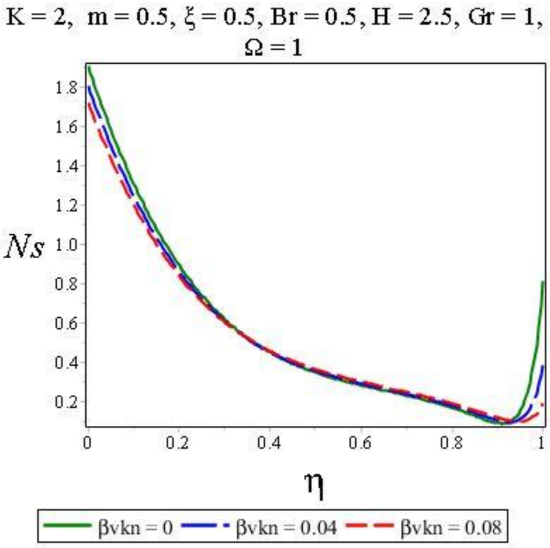

Fig 15: Entropy generation for various values of $\beta_V Kn$

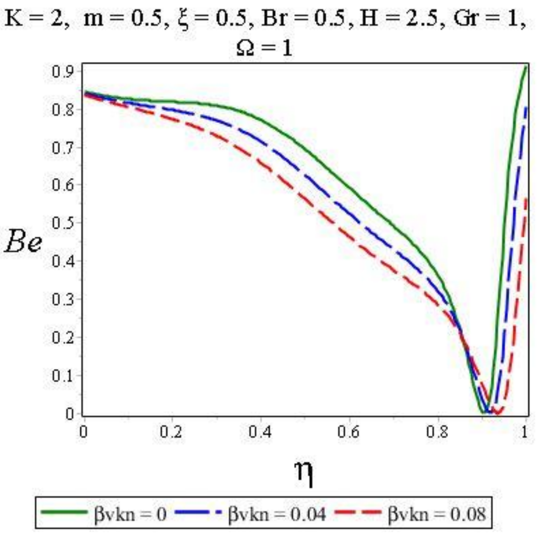

Fig 16: Bejan number for various values of $\beta_V Kn$

Next is the influence of wall-ambient temperature difference ratio (ξ) on fluid motion, fluid temperature, entropy generation and Bejan number. It is noted in Figures 17, 18 and 19 that primary velocity, secondary velocity and fluid temperature are enhanced as wall-ambient temperature difference ratio (ξ) increases. However increase in wall-ambient temperature difference ratio (ξ) reduce the entropy generation and Bejan number as displayed in Figures 20 and 21. This is an indication that fluid friction irreversibility is the major contributor to entropy generation.

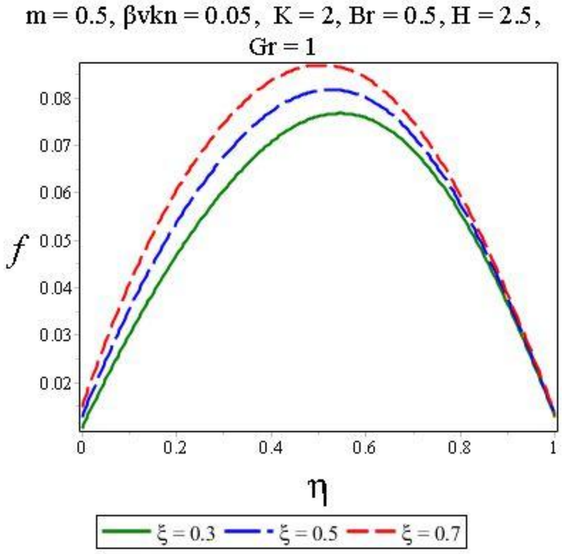

Fig 17: Primary velocity profile for various values of ξ

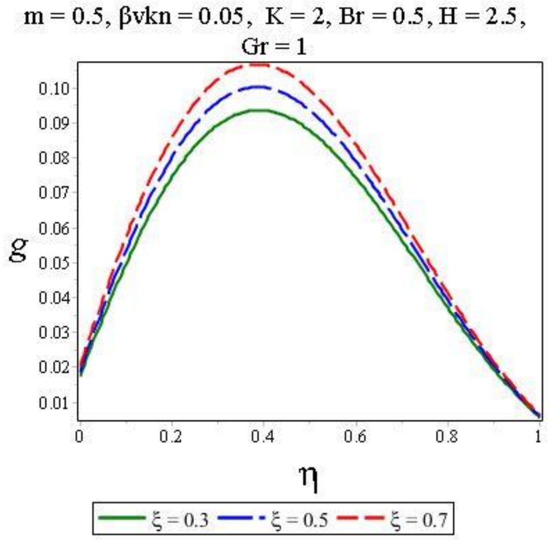

Fig 18: Secondary velocity profile for various values of ξ

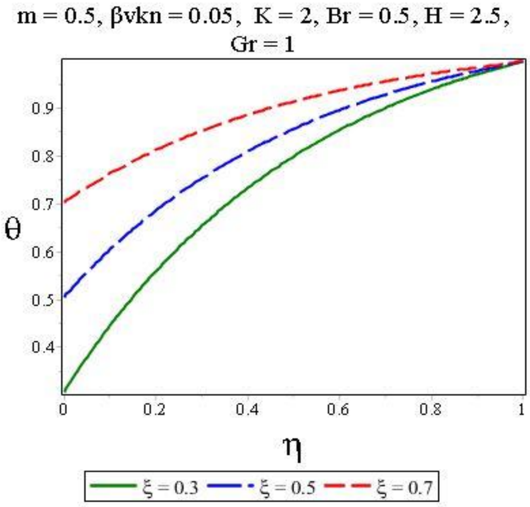

Fig 19: Temperature profile for various values of ξ

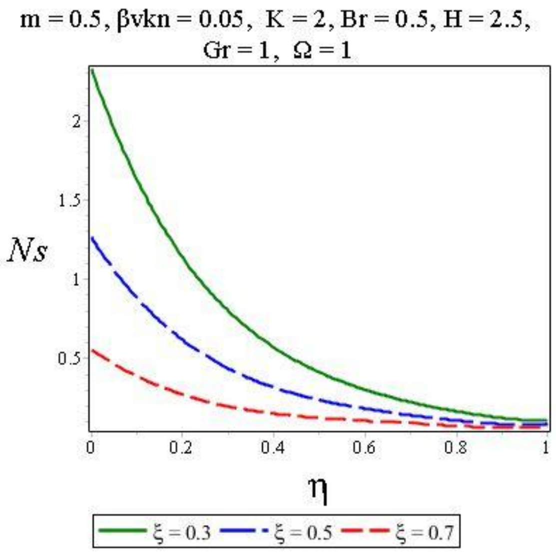

Fig 20: Entropy generation for various values of ξ

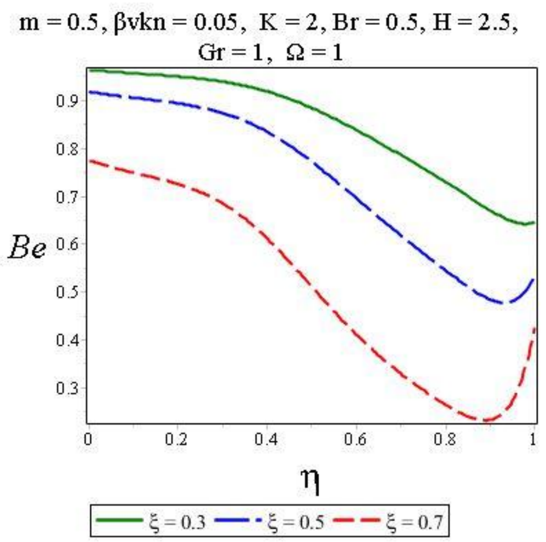

Fig 21: Bejan number for various values of ξ

Furthermore, the effect of Brinkman number on fluid velocity, temperature, entropy generation and Bejan number is display in Figures 22- 26. For various values of Brinkman number (Br) the primary velocity, secondary velocity, fluid temperature and entropy generation in Figures 22, 23, 24 and 25 increase. The term which represents the Brinkman number in the energy equation is a strong source of heat, therefore an increase in Brinkman number increases the velocity, temperature and entropy generation of the fluid. On the other hand it is shown in Figure 26 that Bejan number increases in the region $0 \le \eta < 0.2$ but reduces in the region $0.2 < \eta \le 1$. This indicates that heat irreversibility dominates entropy generation within the interval $0 \le \eta < 0.2$ while fluid friction irreversibility is dominant at $0.2 < \eta \le 1$.

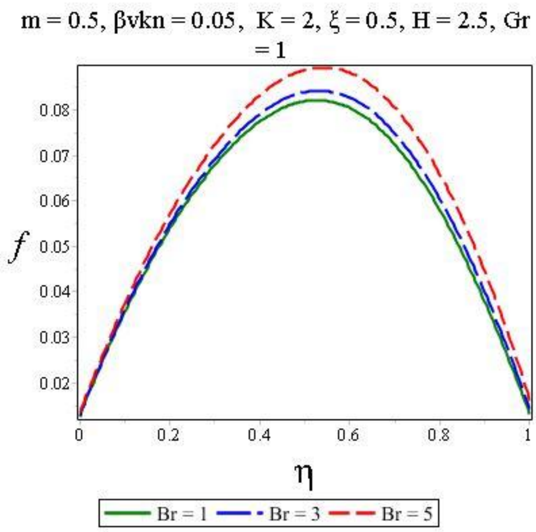

Fig 22: Primary velocity profile for various values of Br

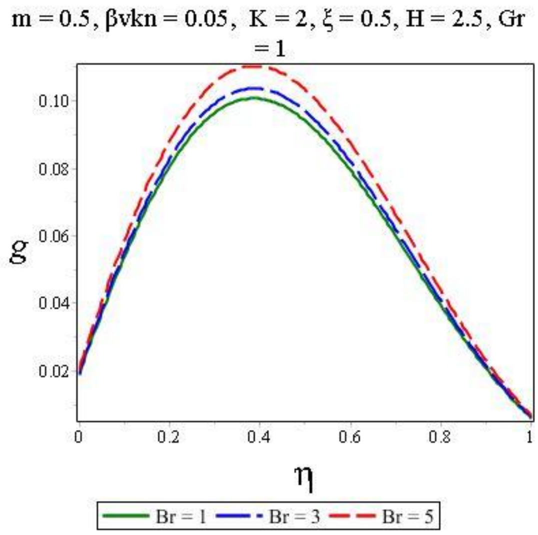

Fig 23: Secondary velocity profile for various values of Br

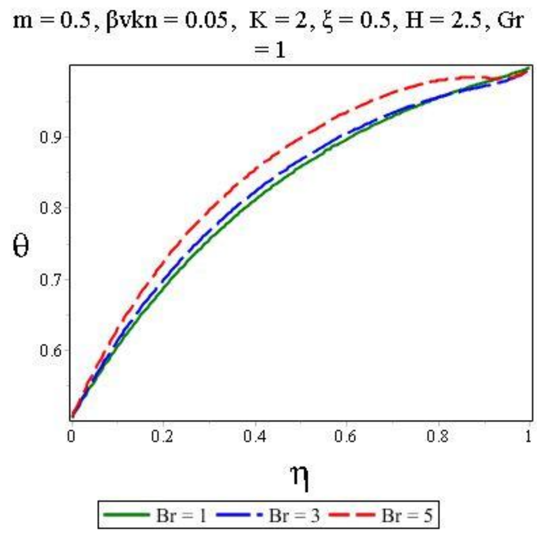

Fig 24: Temperature profile for various values of Br

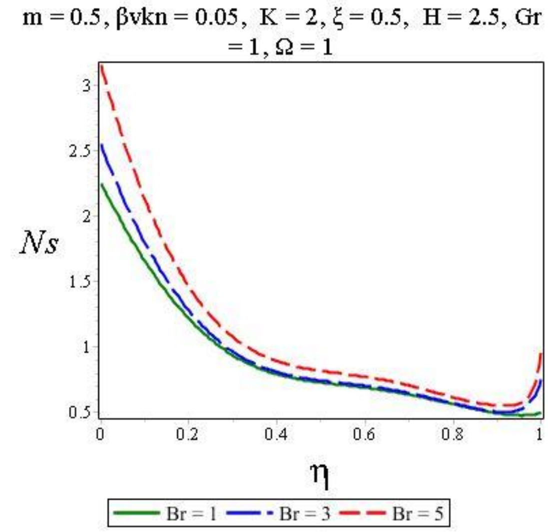

Fig 25: Entropy generation for various values of *Br*

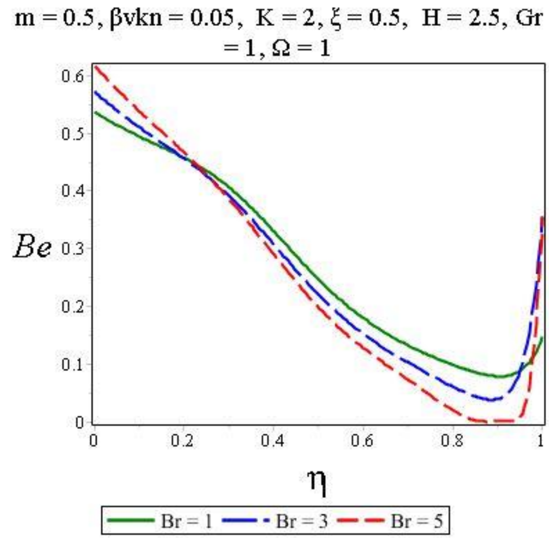

Fig 26: Bejan number for various values of *Br*

The influence of Hartman number is depicted in Figures 27-31. Figures 27 and 28 reveal that fluid velocity is brought under control by increasing the Hartman number. Application of magnetic field in the perpendicular direction to the flow of fluid induces an opposing force in the flow direction, this is as a result of the effect of Lorentz force. The Lorentz force has the tendency to retard fluid motion when the magnetic field value is enhanced. In Figures 29 fluid temperature rises slightly leading to a rise in fluid entropy generation as depicted in Figure 30. A rise in Bejan number is noticed in Figure 31 with increasing values of the magnetic parameter, which is an indication that the entropy generation observed in Figure 30 is contributed by heat transfer irreversibility.

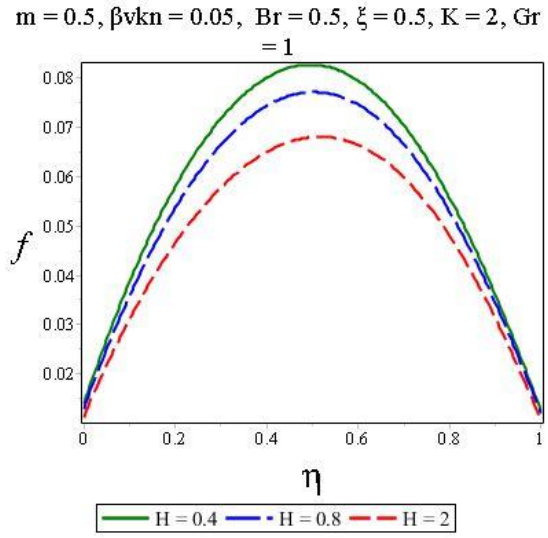

Fig 27: Primary Velocity Profile for various values of *H*

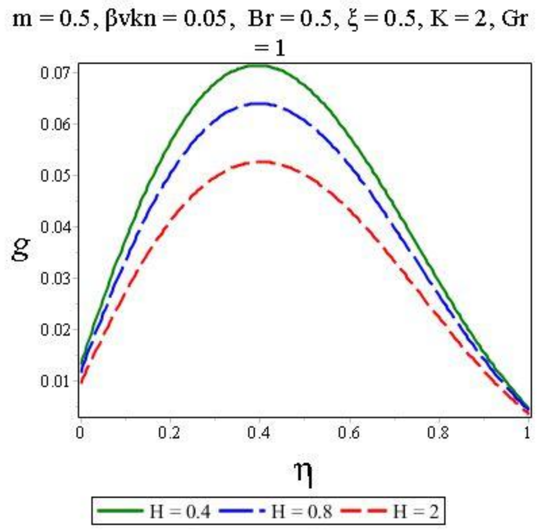

Fig 28: Secondary Velocity Profile for various values of *H*

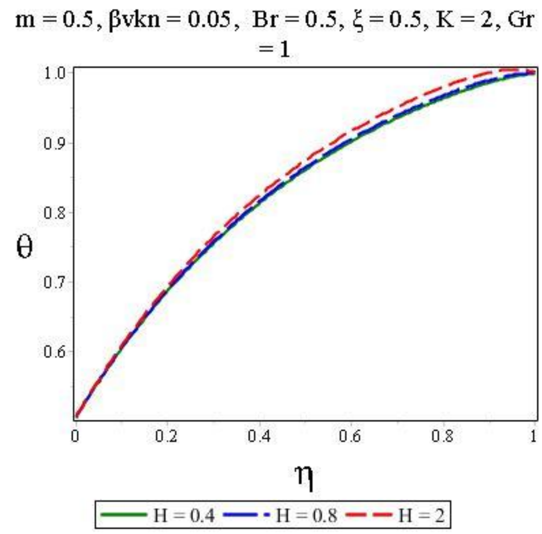

Fig 29: Temperature Profile for various values of *H*

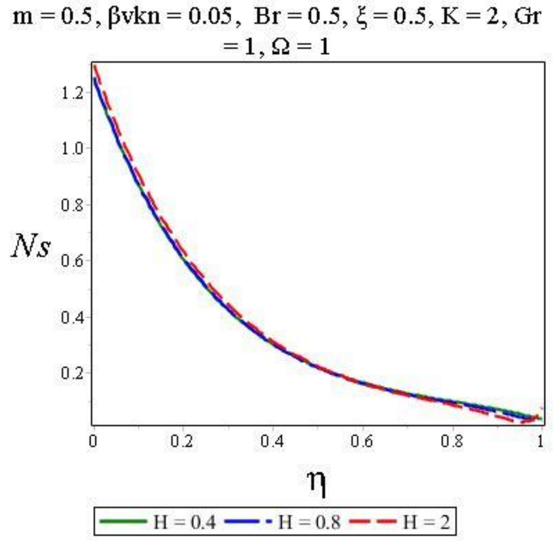

Fig 30: Entropy Generation for various values of H

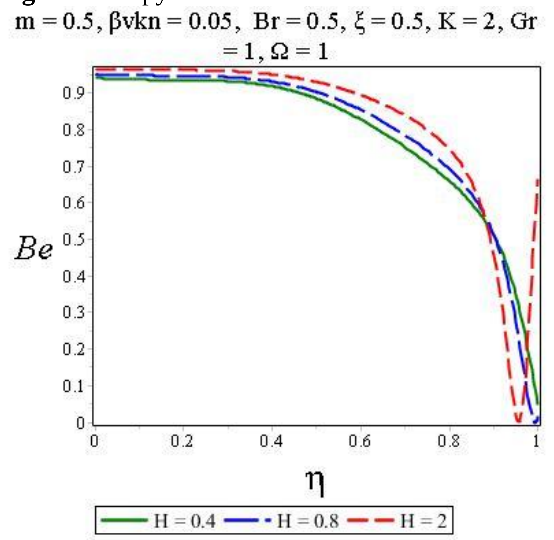

Fig 31: Bejan number for various values of H

Finally, the response of fluid velocity, temperature, entropy generation and Bejan number to a rise in the values of Grashof number is displayed in Figures 32-36. Primary velocity, seocondary velocity, fluid temperature and entropy generation increase with an enhancement in Granshof number as depicted in Figures 32-35, while in Figure 36 Bejan number registers a decrease as Grashof number increases, which indicates that fluid friction irreversibility dominates entropy generation. However a slight rise in Bejan number is noticed at the upper wall of the channel.

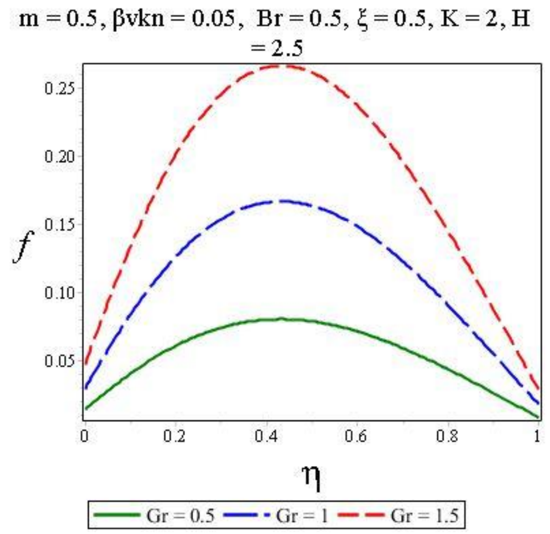

Fig 32: Primary Velocity Profile for various values of Gr

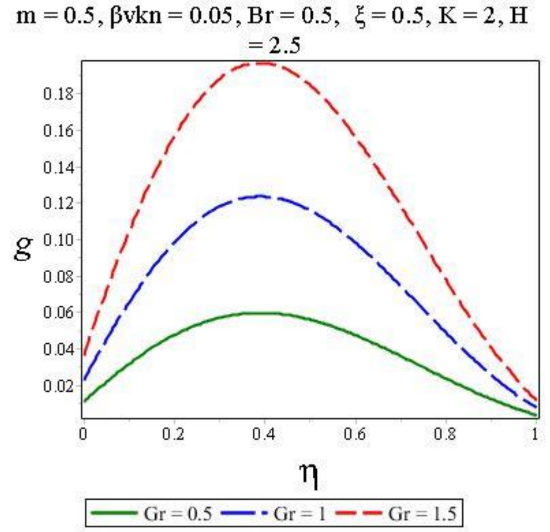

Fig 33: Secondary Velocity Profile for various values of Gr

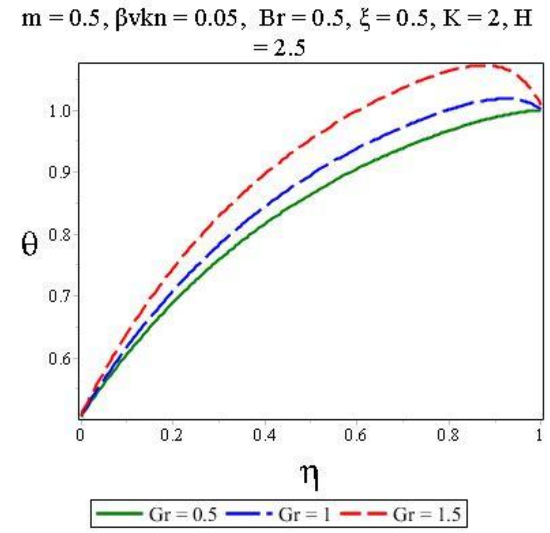

Fig 34: Temperature Profile for various values of Gr

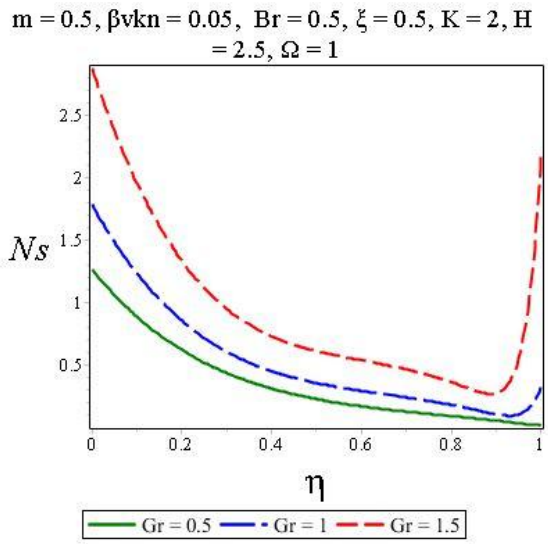

Fig 35: Entropy Generation for various values of Gr

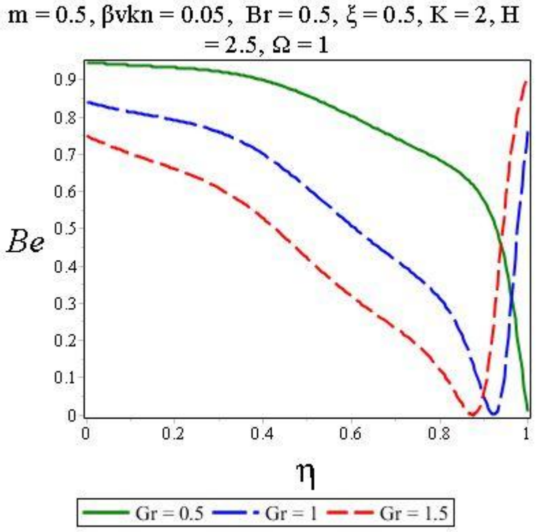

Fig 36: Bejan number for various values of Gr

The numerical values of skin friction $f'(0)$ and $f'(1)$ are presented in Table 3. It is noticed that for a fixed value of m and varying values of Prandtl number from 0.044 (which corresponds to mercury) to 0.71 (corresponding to air) the skin friction $f'(0)$ decreases while $f'(1)$ increases. However the skin friction $f'(0)$ and $f'(1)$ register an increase with a rise in the values of m for a fixed value of Pr.

In Table 4, the values of Nusselt number are entered to depict its response to parameters variation. For a fixed value of m and a rise in Prandtl number the Nusselt number $\theta'(0)$ receives a boost while $\theta'(1)$ decreases. The explanation for this is traced to the dominance of frictional forces at the stationary plate as the value of Prandtl number grows, which increases the rate of heat transfer. Furthermore, increase in m values when Prandtl number in fixed resulted in the reduction of the Nusselt number $\theta'(0)$ while $\theta'(1)$ increases.

Table 3: Skin Friction for different values of Pr and m where $c = 0.25$, $K = 2$, $Gr = 1$, $H = 5$, $\beta_V kn = 0.05$

Pr	m	$f'(0)$	$f'(1)$
0.044	0.1	−0.149124	−0.452826
0.71	0.1	−0.170389	−0.425957
0.71	0.4	−0.167496	−0.225808

Table 4: Nusselt Number for different values of Pr and m where $c = 0.25$, $Br = 1$, $H = 5$, $\xi = 0.5$, $\ln = 0.1$ $\beta_v kn = 0.05$

Pr	m	$\theta'(0)$	$\theta'(1)$
0.044	0.1	0.549974	0.425245
0.71	0.1	1.309208	−0.292143
0.71	0.4	1.305925	−0.284209

V. CONCLUSION

This research work has addressed the entropy generation analysis of unsteady hydromagnetic Couette flow through vertical microchannel with the influence of Hall current and Ion-slip. The resulting non-linear differential equations from the model are solved analytically using differential transform technique. The main summary of this work are outlined below:

- Fluid primary velocity decreases with increase in Hall Current, ion-slip and magnetic field parameters and increases with rarefaction parameter, wall-ambient temperature difference ratio parameter, Brinkman and Grashof numbers,
- Secondary velocity increases with increase in Hall current, ion-slip and rarefaction parameters, wall-ambient temperature difference ratio parameter, Brinkman and Grashof numbers, but is retarded with increase in magnetic field parameter,
- Temperature profile is unaffected by Hall current, however it increases as wall-ambient temperature difference ratio parameter, Brinkman number, magnetic field parameter and Grashof number take higher values. The reverse phenomenon is observed as rarefaction parameter increases,
- Entropy generation is minimised as Hall current, ion-slip, rarefaction and wall-ambient temperature difference ratio parameters increase but increases with a rise in Brinkman number, magnetic field parameter and Grashof number,
- Entropy generation is contributed by both fluid friction and heat transfer irreversibilities.

ACKNOWLEDGMENT

Authors appreciate anonymous reviewers for their invaluable comments.

REFERENCES

[1] G.K. Batchelor, "An introduction to fluid dynamics", Cambridge University Press, 1967.
[2] J. Lopez-Lemus and R.M. Velasco, "Slip boundary conditions in Couette flow", *J. of Physica A*, vol. 274, pp 454 – 465, December, 1999.

[3] B.K. Jha, B.Y. Isah, I.J. Uwanta, “Unsteady MHD free convective Couette flow between vertical porous plates with thermal radiation”, *J. King Saud Univ. – Sci*. vol. 27, pp 338–348, July 2015.

[4] R.N. Jana, N. Datta, B. S. Mazumder, “Magnetohydrodynamic Couette flow and heat transfer in a rotating system”, *J. Phys. Soc. Japan*, vol. 42, pp 1034-1039, March 1977.

[5] G. Bodosa and A.K. Borkakati, “MHD Couette flow with heat transfer between two horizontal plates in the presence of a uniform transverse magnetic field”, *Theoret. Appl. Mech*., vol. 30, no.1, pp 1-9, May 2003.

[6] S. Das, S.L. Maji, M. Guria, R.N. Jana, “Unsteady MHD Couette flow in rotating system”, *Math. Comp. Modelling*, vol. 50, pp 1211-1217, 2009.

[7] S. Guchhait, S. Das, R.N. Jana, S.K. Ghosh, “Combined effects of Hall current and rotation on unsteady Couette flow in porous channel”, *World J. Mech*. vol. 1, pp 87-99, May 2011.

[8] B.K. Jha, C.A. Apere, “Hall and ion-slip effects on unsteady MHD Couette flow in a rotating system with suction and injection”, *J. Phys. Soc. Japan*, vol. 80. October 2011 DOI:10.1143/JPSJ.80.114401

[9] S.K. Gosh, O.A. Beg, M. Narahari, “A study of unsteady rotating hydromagnetic free and forced convection in a channel subject to forced oscillation under an oblique magnetic field”, *J. Appl. Fluid Mech*. vol. 6, no. 2, pp 213–227, 2013.

[10] G.S. Seth, B. Kumbhakar, R. Sharma, “Unsteady hydromagnetic natural convection flow of a heat absorbing fluid within a rotating vertical channel in porous medium with Hall effects”, *J. Appl. Fluid Mech*. vol. 8, no. 4, pp 767–779, 2015.

[11] G.S. Seth, R.N. Jana, M.K. Maiti, “Unsteady hydromagnetic Couette flow in a rotating System”, *Int. J. Engng. Sci*. vol. 20, no. 9, pp 989-999, 1982.

[12] G.S. Seth, Md. S. Ansari, R. Nandkeolyar, “Unsteady hydromagnetic Couette flow induced due to accelerated movement of one of the porous plates of the channel in a rotating system”, *Int. J. Appl. Math. Mech*. vol. 6, no. 7, pp 24- 42, January 2010.

[13] A.O. Ajibade, A.M. Umar, “Effect of chemical reaction and radiation absorption on the unsteady MHD free convection Couette flow in a vertical channel filled with porous materials”, *Afr. Mat*. vol. 27, pp 201–213, May 2015. DOI 10.1007/s13370-015-0334-7

[14] K.D. Singh, R. Pathak, “Effect of rotation and Hall current on mixed convection MHD flow through a porous medium filled in a vertical channel in presence of thermal radiation”, *Indian Journal of Pure and Applied Physics*, vol. 50, 77-85, February 2012.

[15] A.R. Hassan, J.A. Gbadeyan, “The Effect of Heat Absorption on a Variable Viscosity Reactive Couete Flow under Arrhenius Kinetics”, *Theoretical Mathematics & Applications*, vol. 3, no. 1, pp 145-159, April 2013.

[16] S. Das, R.N. Jana, O.D. Makinde, “Transient hydromagnetic reactive Couette flow and heat transfer in a rotating frame of reference”, *Alexandria Engineering Journal*, vol. 55, pp 635–644, March 2016.

[17] N.S. Kobo, O.D. Makinde, “Second law analysis for a variable viscosity reactive Couette flow under Arrhenius kinetics”, *Math. Probl. Eng*. pp 1–15, May 2010.

[18] H.C. Weng, C.K. Chen, “Variable physical properties in natural convective gas microflow”, *J. Heat Transf.* vol. 130, no. 8, May 29, 2008. doi:10.1115/1.2927400

[19] S.O. Adesanya, “Free convective flow of heat generating fluid through a porous vertical channel with velocity slip and temperature jump”, *Ain Shams Eng J.* February 2015, http://dx.doi.org/10.1016/j.asej.2014.12.008

[20] B.K. Jha, B. Aina, S.B. Joseph, “Natural convection flow in vertical Micro-channel with Suction/Injection”, *J. Process Mech. Eng*. vol. 228, no. 3, pp 171–180, July 2013.

[21] S. Yu, T.A. Ameel, “Slip-flow heat transfer in rectangular microchannels”. *Int J Heat Mass Transfer*, vol. 44, no. 22, pp 4225-4234, Nov. 2001.

[22] A.F. Khadrawi, A. Othman, M.A. Al-Nimr, “Transient free convection fluid flow in a vertical microchannel as described by the hyperbolic heat conduction model”. *Int J Thermophys*, vol. 26, no. 3, pp 905–18, May 2005.

[23] L. Biswal, S.K. Som, S. Chakraborty S. “Effects of entrance region transport processes on free convection slip flow in vertical microchannels with isothermally heated walls”. *Int J Heat Mass Transfer*, vol. 50, no. 12, pp 48–54, April 2007.

[24] C.K. Chen, H.C. Weng, “Developing natural convection with thermal creep in a vertical microchannel”. *J Phys D*, vol. 39, no. 3, pp 107–18, 2006.

[25] A.A. Opanuga, O.O. Agboola, H.I. Okagbue and S.A. Bishop, “Convection flow of MHD couple stress fluid in vertical microchannel with entropy generation, Pattern Formation and Stability in Magnetohydrodynamics”, November 2018. DOI: http://dx.doi.org/10.5772/intechopen.81123.

[26] O.O. Agboola, A.A. Opanuga, H.I. Okagbue, S.A. Bishop, P.O. Ogunniyi, “Analysis of Hall effects on the entropy generation of natural convection flow through a vertical microchannel”, *International Journal of Mechanical Engineering and Technology (IJMET)*, vol. 9, no. 8, pp 712–721, August 2018.

[27] A. Bejan, “Entropy Generation through Heat and Fluid Flow”, Wiley, New York, 1982.

[28] S. Das and R.N. Jana, “Entropy generation due to MHD flow in a porous channel with Navier slip”, *Ain Shams Engineering Journal*, vol. 5, pp 575-584, December 2013.

[29] A. Arikoglu, I. Ozkol, and G. Komurgoz, “Effect of slip on entropy generation in a single rotating disk in MHD flow”, *Applied Energy*, vol. 85, pp 1225–1236, December 2008.

[30] S.O. Adesanya, O.D. Makinde, “Irreversibility analysis in a couple stress film flow along an inclined heated plate with adiabatic free surface”, *Physica A*, vol. 432, pp. 222–229, February 2015.

[31] S.O. Adesanya and J.A. Falade, “Thermodynamics analysis of hydromagnetic third grade fluid flow through a channel filled with porous medium”, *Alexandria Engineering Journal*, vol. 54, pp 615–622, December 2015.

[32] A.O. Ajibade, B.K. Jha, and A. Omame, “Entropy generation under the effect of suction/injection”, *Applied Mathematical Modelling*, vol. 35, pp 4630–4646, March 2011.

[33] M. Bouabid, M. Magherbi, N. Hidouri 1 and A. B. Brahim, “Entropy generation at natural convection in an inclined rectangular cavity”, *Entropy*, vol. 13, pp 1020-1033, May 2011.

[34] M. Mehdi Rashidi and N. Freidoonimehr, “Effects of velocity slip and temperature jump on the entropy generation in MHD flow over a porous rotating disk”, *Journal of Mechanical engineering*, vol. 1, no. 3, pp 3-14, November 2012.

[35] Abiodun A. Opanuga, Jacob A. Gbadeyan, and Samuel A. Iyase, "Second Law Analysis of Hydromagnetic Couple Stress Fluid Embedded in a Non-Darcian Porous Medium," IAENG International Journal of Applied Mathematics, vol. 47, no.3, pp287-294, August 2017

[36] A.A. Opanuga, J.A. Gbadeyan, O.O. Agboola, H.I. Okagbue, “Effect of suction/injection on the entropy generation of third grade fluid with convective cooling”, *Defect and Diffusion*, vol. 384, pp 21-30, May 2018.

[37] A.A. Opanuga, H.I. Okagbue, O.O. Agboola, O.F. Imaga, “Entropy generation analysis of buoyancy effect on hydromagnetic Poiseuille flow with internal heat generation”, *Defect and Diffusion*, vol. 378, pp 102-112, July 2017. doi:10.4028/www.scientific.net/DDF.378.102.

[38] A.A. Opanuga, H.I. Okagbue, O.O. Agboola, S.A. Bishop, “Second law analysis of Ion slip effect on MHD couple stress fluid”, *International Journal of Mechanics*. vol. 12, pp 96-101, June 2018.

[39] S. Sirisubtawee, "Comparison of Analytical and Numerical Solutions of Fractional-Order Bloch Equations using Reliable Methods," Lecture Notes in Engineering and Computer Science: Proceedings of The World Congress on Engineering 2018, WCE 2018, 14 March - 16 March, 2018, Hong Kong, China, pp 467-472.

[40] N. Lekdee, S. Sirisubtawee, S. Koonprasert, "Exact Solutions and Numerical Comparison of Methods for Solving Fractional-Order Differential Systems," Lecture Notes in Engineering and Computer Science: Proceedings of The World Congress on Engineering 2018, WCE 2018, 14 March - 16 March, 2018, Hong Kong, China, pp. 459-466

[41] W. Khongtham, "Solution of Fractional Gas Dynamic Equation by Using Homotopy Perturbation with Natural Transform Method," Lecture Notes in Engineering and Computer Science: Proceedings of The World Congress on Engineering 2018, WCE 2018, 4 July - 6 July, 2018, London, U.K., pp. 60-62

[42] P. Klankaew, N. Pochai, "Numerical Simulation of a Nonlinear Thin Fluid Film Flow Velocity Model of a Third Grade Fluid on a Moving Belt using Finite Difference Method with Newton Iterative Scheme," Lecture Notes in Engineering and Computer Science: Proceedings of The World Congress on Engineering 2019, WCE 2019, 13 March - 15 March, 2019, Hong Kong, China, pp.318-321.

[43] L.M. Jiji, “Heat Convection”, first ed., Springer, New York, 2006.